PICOSECOND KINETIC ABSORPTION AND FLUORESCENCE STUDIES OF BOVINE RHODOPSIN WITH A FIXED 11-ENE

J. Buchert, V. Stefancic, A. G. Doukas, R. R. Alfano, R. H. Callender, and J. Pande
Physics Department, The City College of The City University of New York, New York, New York 10031

H. Akita, V. Balogh-Nair, and K. Nakanishi
Department of Chemistry, Columbia University, New York, New York 10027

ABSTRACT   A synthetic retinal having a fixed 11-*cis* geometry has been used to prepare a nonbleachable analogue of bovine rhodopsin. Marked differences in the picosecond absorption and fluorescence behavior of this analogue at room temperature, compared with that of natural rhodopsin, were observed. This not only indicates that the 11-*cis* to *trans* isomerization of the retinal moiety is the crucial primary event in the photolysis of rhodopsin, but also it establishes that this isomerization must occur on the picosecond time scale or faster.

INTRODUCTION

The visual pigment, rhodopsin, consists of a chromophore 11-*cis* retinal covalently bound to a protein through a protonated Schiff base. A great deal of evidence suggests that the action of light on visual pigments is to isomerize the 11-*cis* retinal to an all-*trans* form, although a number of alternative models have been proposed (see recent reviews of Ottolenghi, 1980, and Balogh-Nair et al., 1982). One test of the various models involves experiments on an artificial rhodopsin in which the 11-*cis* retinal chromophore has been replaced by an 11-*cis* analogue where C = 10 and C = 13 of the retinal polyene backbone have been bridged by a three-carbon alkyl group (Fig. 1) (Akita et al., 1980). This retinal analogue forms a pigment absorbing at 490 nm, which is quite close to the 500 nm maximum of rhodopsin; this suggests that the analogue interacts with the apoprotein in a manner similar to that of native 11-*cis* retinal, although small changes in the protein environment of the chromophore to accommodate the alkane ring are possible. The three-carbon alkyl bridge, however, prevents isomerization about the 11-12 double bond. We call this artificial rhodopsin Rh7, which denotes formation of the seven-membered carbocyclic ring.

We examine here the room-temperature picosecond absorption and fluorescence kinetic behavior of bovine Rh7 to compare its kinetic properties with rhodopsin. Rhodopsin exhibits quite simple picosecond kinetic behavior

(Busch et al., 1972; Monger et al., 1979; Kobayashi, 1980; Doukas et al., 1981). A species called bathorhodopsin (absorption maximum = 543 nm) is formed photochemically from rhodopsin in <6 ps and thermally decays to a third species (lumirhodopsin) on the nanosecond time scale. We find that the picosecond kinetic behavior of Rh7 is very different from that of rhodopsin. This is in agreement with earlier findings that, in contrast to the behavior of natural rhodopsin, no detectable photochemistry was observed for Rh7 in microsecond flash photolysis experiments at room temperature or in irradiation studies at 77 K (Mao et al., 1981). We conclude that isomerization of the retinal moiety is a crucial step in the photolysis of rhodopsin. In addition, our experiments show that the isomerization must happen on the picosecond time scale or faster.

METHODS AND MATERIALS

The synthesis of the retinal analogue (Fig. 1 *b*) and its incorporation into bovine opsin has been previously described (Akita et al., 1980). The purified artificial rhodopsin was solubilized in a 2% digitonin/67 mM phosphate buffer, pH7.0, to an optical density at the absorption maximum of ~2.5–3.0 OD/cm.

The picosecond absorption system has been fully described elsewhere (Monger et al., 1979). A six-ps, 530-nm second harmonic of a Nd^{3+} glass laser was used as the actinic pulse. This 530 nm pulse was also used to generate 8-ps continuum radiation from CCl_4 in the range of 400–800 nm. Radiation at various frequencies was extracted from this continuum radiation using narrow band-pass filters and was variably time delayed with respect to the actinic pulse. This radiation spatially overlapped the actinic light incident on the sample, and changes in the transmission of the probe pulse through the sample were monitored. The time resolution was ~10 ps. A typical actinic 530-nm pulse incident on the sample was 1.5 × $10^{-2} cm^2$ in size, and had a density of 2 × 10^{16} photons/cm^2. Typical size
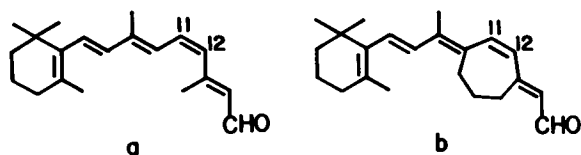
FIGURE 1 Structural diagrams of (a) 11-cis retinal and (b) synthetic analogue with fixed 11-ene configuration.

of the probe pulse was 5×10^{-3} cm^2, and its density was 2×10^{13} photons/cm^2.

The picosecond fluorescence spectrometer has also been detailed elsewhere (Yu et al., 1977; Doukas et al., 1982). A single 6-ps, 527 nm pulse was used to excite the sample. The spot size of the exciting pulse was 1.5×10^{-2} cm^2 at the sample position. Various power densities from 2×10^{15} to 2×10^{16} photons/cm^2 were used, and all gave similar results. The sample was frontally excited, and the fluorescence collected and focused onto a 30-μm entrance slit of a Hamamatsu streak camera (Hamamatsu Corp., Middlesex, NJ) for temporal analysis. Various narrow band-pass filters were placed in the path of the fluorescence to isolate selected wavelengths of the fluorescence. A 550-nm cutoff filter (model 3-67, Corning Glass Works, Corning Medical and Scientific, Corning, NY) was also placed in the fluorescence path to eliminate any scattered laser light. A 527-nm prepulse was used to provide a reference on the time axis for signal averaging. The streak camera was coupled to a GBC SIT video camera and temporal analyzer (Night Vision Camera, New York, NY). This was interfaced to a Digital Equipment Corp. (DEC) minc minicomputer, and the data transferred from the minc minicomputer to a DEC PDP/10 computer for analysis (Digital Equipment Corp., Marlboro, MA). The data were corrected for nonlinearities of the streak camera both in time and intensity. The time resolution (FWHM) of the complete apparatus (laser plus streak camera) was measured to be 12 ps.

Standard least-square fitting procedures using exponential functions were used to determine the rise times and decay times of the absorption and fluorescence. All time constants were defined to be the time from the maximum to the $1/e$ points. The quantum yields of fluorescence were determined by measuring the fluorescence of a solution of erythrosin of the same optical density as the Rh7 samples under otherwise identical conditions. Corrections were made for the difference of the absorbances of the two samples, and a previously measured value of erythrosin's quantum yield of 0.02 was used (Bowers and Porter, 1967).

RESULTS AND CONCLUSIONS

The absorbance changes observed from Rh7 at several wavelengths on the picosecond time scale after excitation by a single 6 ps 530-nm actinic pulse, are shown in Fig. 2. Near the absorption maximum of Rh7 at 470 nm, a fast unresolved (<10 ps) depletion (negative absorbance changes) of the ground state, followed by what appears to be biphasic recovery consisting of a fast unresolved component and a slower 50 ± 10 ps component (Fig. 2 a) was seen. Although the biphasic nature of the recovery is barely evident within our signal-to-noise ratio, three separate measurements at 470 nm gave the same behavior. Positive absorbance changes are observed at 570 nm (Fig. 2 b) and at 640 nm (Fig. 2 c). The 570 nm species, Rh7(570), is formed in <10 ps and decays in 20 ± 10 ps. The 640 nm species, Rh7(640), is formed in 20 ± 10 ps and decays in 50 ± 10 ps. Because the decay time of Rh7(570) matches the formation time of Rh7(640), it is reasonable to conclude
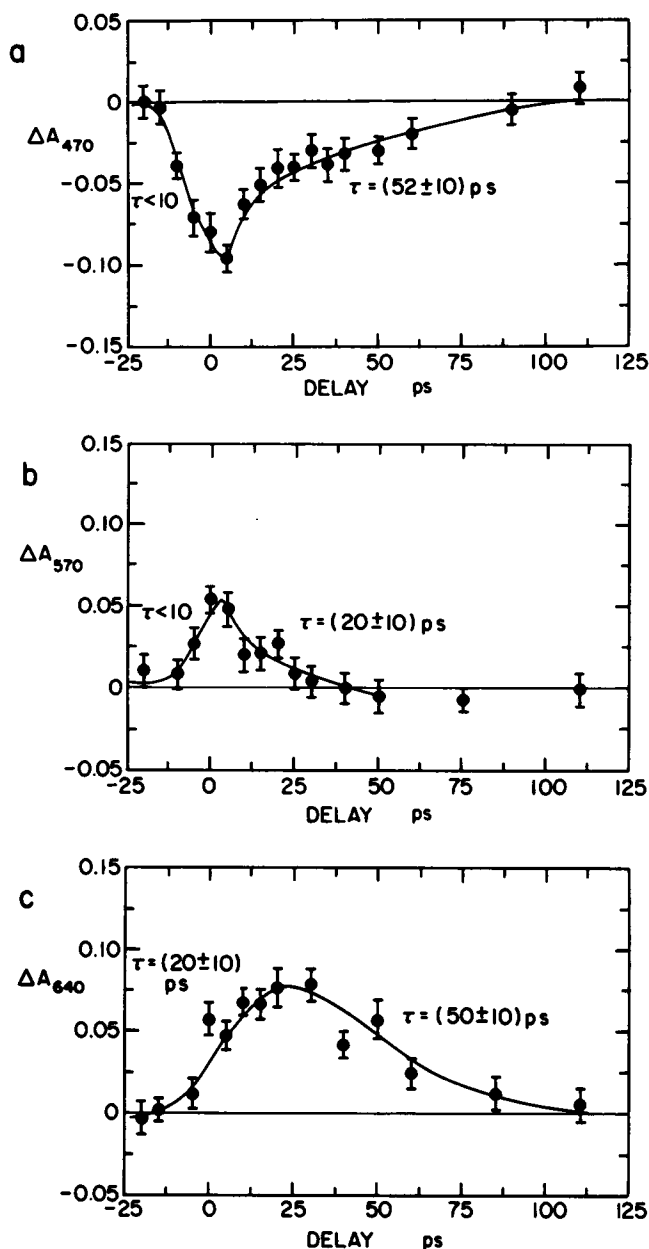

FIGURE 2 Laser-induced absorbance changes for the seven-member visual pigment at room temperature, excited by a single 530-nm pulse at (a) λ – 470 nm, (b) λ – 570 nm, (c) λ – 640 nm as a function of time delay.

that Rh7(640) is formed from Rh7(570). Likewise, the repopulation kinetics of Rh7 observed at 470 nm match the decay of Rh7 (640) within our signal-to-noise ratio.

The picosecond fluorescence kinetic properties of Rh7 are summarized in Fig. 3. A resolvable fluorescence fast component with a rise time of 25 ± 12 ps and a decay time of 55 ± 10 ps is observed (Fig. 3 a). A second, slower component is also evident that has a decay time of 900 ± 50 ps. The "slow" component is similar in its kinetic properties to that observed in our previous fluorescence

a

FLUORESCENCE INTENSITY (arbitrary units)

$\tau_R = (25 \pm 10)$ ps

$\tau_D = (55 \pm 10)$ ps

$\tau = (900 \pm 50)$ ps

125 ps

TIME   ps

b

FLUORESCENCE INTENSITY (arbitrary units)

$\lambda_F = 560$ nm

200 ps

TIME   ps

c

FLUORESCENCE INTENSITY (arbitrary units)

$\lambda_F = 650$ nm

200 ps

TIME   ps
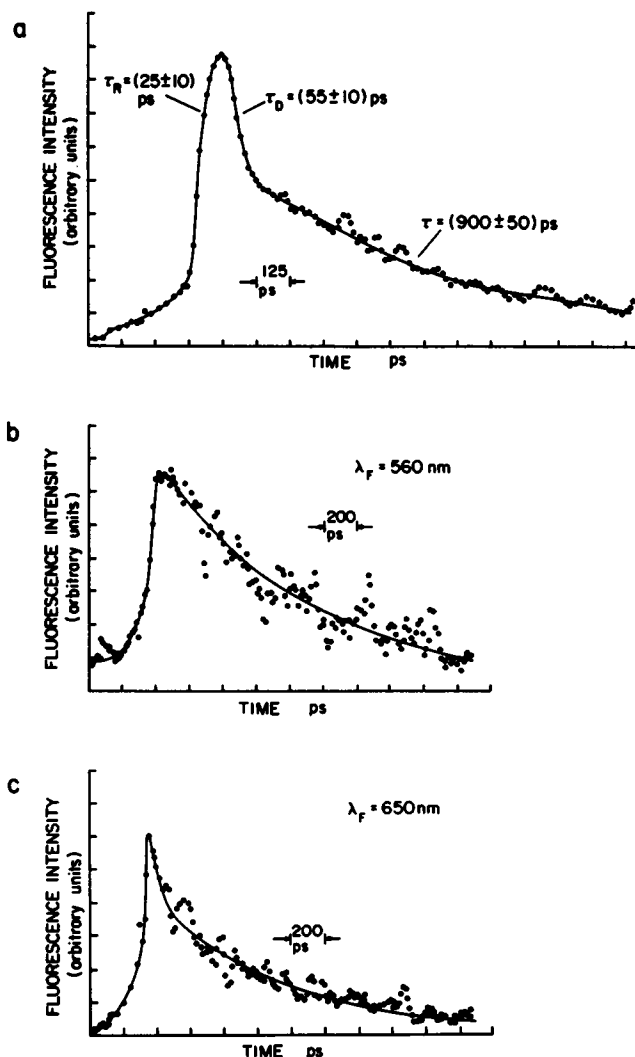
FIGURE 3 Fluorescence kinetics of seven-membered visual pigment at room temperature, excited by a single 527-nm pulse for (a) λ — 550–700 nm, (b) λ — 560 nm, (c) λ — 650 nm.

studies of rhodopsin, isorhodopsin, and bleached rhodopsin (Doukas et al., 1981). As in that report, we ascribe the slow component to sample impurities. Fig. 3, b and c, shows the fluorescence signal at 560 and 650 nm, respectively. As can be seen, the fast fluorescent component is very small at 560 nm while the slow component signal is relatively weaker at 650 nm. Fig. 4 shows the emission profile of the fast and slow components. The rise and decay times of the fast fluorescent component match quite well the formation and decay of the Rh7(640) species. It is reasonable to assign the fast fluorescence to Rh7(640) from this close match of kinetic times, although other interpretations are possible (accidental impurity emission, for example). Our major conclusions discussed below do not depend on this assignment, but the strong inference from the data is that Rh7(640) is an excited state species. The quantum yield of the fast component is ~4 × 10⁻⁴.

The data suggest a rather simple kinetic scheme:

<10 ps   <10 ps   20 ps

Rh7 (490) $\xrightarrow{\text{wwv}}$ Rh7* ___ Rh7 (570)* ___ Rh7 (640)*

<10 ps

50 ps
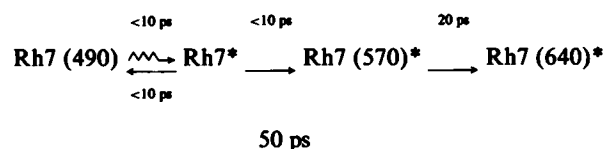
Scheme I

where straight lines indicate thermal reactions, wavy lines indicate the photo reaction, and the asterisk indicates an excited-state species. The numbers in parentheses indicate aborption maxima (only very approximately for the 570 and 640 nm species, since only a single probe wavelength was used). Rh7* has been included in this scheme to denote the vertically excited Frank-Condon state of Rh7. That Rh7* and Rh7(570)* are not the same species can be deduced by the following argument. If Rh7(570)* is the vertically excited Frank-Condon state, we should have been able to observe fluorescence from this state. Assuming a radiative time (t_r) of ~5 × 10⁻⁹ s for the vertically excited Frank-Condon state, based on the absorption coefficient of rhodopsin and an observed nonradiative lifetime (t_n) of 20 ps for Rh7(570)*, there should be a quantum
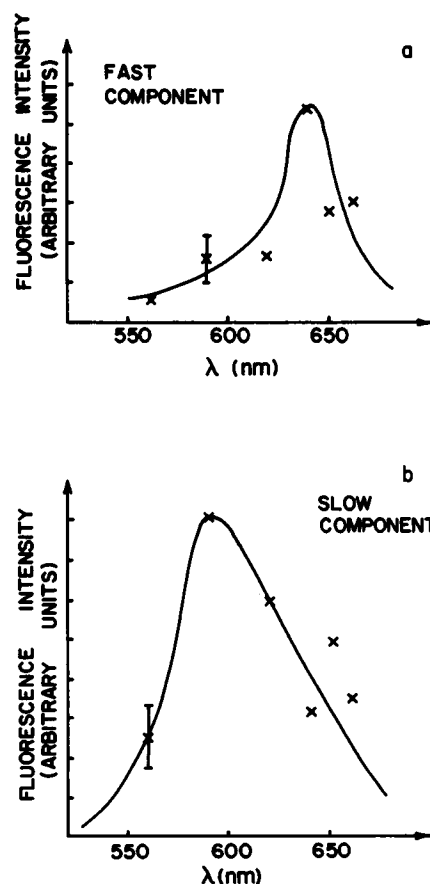

FLUORESCENCE INTENSITY (ARBITRARY UNITS)

FAST COMPONENT   a

550   600   650

λ (nm)

FLUORESCENCE INTENSITY (ARBITRARY UNITS)

SLOW COMPONENT   b

550   600   650

λ (nm)

FIGURE 4 The fluorescence profile of (a) the fast component and (b) the slow component.

yield (QE) of 4×10^{-3} from the relationship $QE = t_n/t_r$. No detectable fluorescence was observed from Rh7(570)*, and we estimate an upper limit of 1×10^{-4} for its quantum yield, 40 times smaller than the predicted value. We thus make the distinction between Rh7*, the vertically excited state, and Rh7(570)*. Using $QE = t_n/t_r$ and the upper limit of QE of 10^{-4} for Rh7, the nonradiative lifetime of Rh7* can be estimated to be <0.5 ps. We elaborate on the meaning of such short lifetimes in another publication (Doukas, Jannakar, Chandra, Buchert, Alfano, Callender, Kakitani, and Honig, in preparation).

The absorption and fluorescence kinetic behavior of rhodopsin is markedly different than Rh7. The only observed species formed photochemically from rhodopsin is bathorhodopsin (absorption maximum = 543 nm; formation time is <6 ps), and bathorhodopsin is stable at room temperature for nanoseconds. Furthermore, bathorhodopsin is a ground-state species, unlike Rh7(570)* or Rh(640)*, since bathorhodopsin is stable at around 100 K or lower for indefinite periods. (It should be noted that our analysis indicates the absorption profile of Rh7(570)* arises from an excited state to excited state transition. Thus, the close match of absorption maxima between Rh7(570)* and bathorhodopsin is fortuitous in this case.)

We conclude that isomerization is an essential component in the rhodopsin-to-bathorhodopsin photoreaction. The π electron systems of the chromophore of Rh7 and rhodopsin are essentially identical, so that all photochemical processes other than 11-cis to trans isomerization could take place. For example, processes such as proton or electron transfers, which have been suggested (van der Meer et al., 1976; Peters et al., 1977; Huppert et al., 1977; Warshel, 1978) in the rhodopsin-to-bathorhodopsin reaction, should not be affected by the incorporation of the three-carbon bridge along the polyene backbone of retinal. Furthermore, the photoreaction pathway available to Rh7, i.e., the formation of Rh7(570)* and Rh7(640)*, is presumably available to the chromophore of rhodopsin. Thus, the data also suggest that the 11-cis to trans isomerization that occurs in the rhodopsin-to-bathorhodopsin phototransition occurs on the picosecond time scale or faster to efficiently compete with the Rh7(560)* and Rh7(640)* pathway. Our results are then entirely consistent with the notion that the effect of light absorption by rhodopsin is to produce an 11-cis to trans photoisomerization of the retinal chromophore in the formation of bathorhodopsin.

We may speculate on the nature of the Rh7(570)* and Rh7(640)* species. Torsional rotations about the polyene bond structure in the excited state manifold are likely candidates for the conformation of these two short-lived states. On experimental grounds, the tendency for retinal chromophores in visual pigments and bacteriorhodopsin to photoisomerize quickly (on the picosecond time scale) about ground-state double bonds appears to be well established from a number of points of view, including the results from this study. The 11-cis photoisomerization in

the rhodopsin-to-bathorhodopsin photoreaction, the 9-cis photoisomerization in the isorhodopsin-(an artificial visual pigment based on a 9-cis retinal chromophore) to-bathorhodopsin photoreaction, and the 13-cis photoisomerization in the light adapted bacteriorhodopsin to K photoreaction are just a few examples. In addition, theoretical considerations are entirely consistent with such fast torsional motions (Honig et al., 1979; see review in Birge, 1981). In our case, the three-membered carbon bridge prevents a major torsional motion about the retinal 11-12 bond; space-filling models and theoretical calculations (Doukas, Jannakar, Chandra, Buchert, Alfano, Callender, Kakitani, and Honig, in preparation; Birge, private communication) show that some rotation is possible about the 11-12 bond even with the seven-member ring retinal of Fig. 1. Thus, it is very plausible that the metastable conformation of the Rh7(570)* and Rh7(640)* states involves torsional rotations of one or more of the retinal polyene bonds, including possibly some rotation about the 11-12 double bond.

REFERENCES

Akita, H., S. P. Tanis, M. Adams, V. Balogh-Nair, and K. Nakanishi. 1980. Nonbleachable rhodopsin retaining the full natural chromophore. J. Am. Chem. Soc. 102:6370–6372.

Balogh-Nair, V., and K. Nakanishi. 1982. New Comprehensive Biochemistry. Stereochemistry. Ch. Tamm, editor. Elsevier/North Holland Amsterdam. 3:283–334.

Birge, R. 1981. Photophysics of light transduction in rhodopsin and bacteriorhodopsin. Annu. Rev. Biophys. Bioeng. 10:315–354.

Bowers, P. G., and G. Porter. 1967. Triplet state quantum yields for some aromatic hydrocarbons and xanthene dyes in dilute solution. Proc. R. Soc. Ser. A299:348–352.

Busch, G. E., M. L. Applebury, A. A. Lamola, and P. M. Rentzepis. 1972. Formation and decay of prelumirhodopsin at room temperatures. Proc. Natl. Acad. Sci. USA. 69:2802–2806.

Doukas, A. G, P. Y. Lu, and R. R. Alfano. 1981. Fluorescence relaxation kinetics from rhodopsin and isorhodopsin. Biophys. J. 35:547–550.

Doukas, A. G., J. Buchert, and R. R. Alfano. 1982. Picosecond laser techniques and design. In Biological Events Probed by Ultrafast Laser Spectroscopy. R. R. Alfano, editor. Academic Press Inc., New York. 17:387–416.

Green, B. H., T. G. Monger, R. R. Alfano, B. Aton, and R. H. Callender. 1977. Cis-trans isomerization in rhodopsin occurs in picoseconds. Nature (Lond.). 269:179–180.

Honig, B., T. Ebrey, R. H. Callender, U. Dinur, and M. Ottolenghi. 1979. Photoisomerization, energy storage, and charge separation: a model for light energy transduction in visual pigments and bacteriorhodopsin. Proc. Natl. Acad. Sci. USA. 76:2503–2507.

Huppert, D., P. Rentzepis, and D. Kliger. 1977. Picosecond and nanosecond isomerization kinetics of protonated 11-cis retinylidene Schiff bases. Photochem. Photobiol. 25:193–197.

Kobayashi, T. 1980. Existence of hypsorhodopsin as the first intermediate in the primary photochemical process of cattle rhodopsin. Photochem. Photobiol. 32:207–215.

Mao, B., M. Tsuda, T. G. Ebrey, H. Akita, V. Balogh-Nair, and K. Nakanishi. 1981. Flash photolysis and low temperature photochemistry of bovine rhodopsin with a fixed 11-ene. *Biophys. J.* 35:543–546.

Monger, T. G., R. R. Alfano, and R. H. Callender. 1979. Photochemistry of rhodopsin and isorhodopsin investigated on picosecond time scale. *Biophys. J.* 27:105–116.

Ottolenghi, M. 1980. The photochemistry of rhodopsin. *Adv. Photochem.* 12:97–200.

Peters, K., M. L. Applebury, and P. M. Rentzepis. 1977. Primary photochemical event in vision: proton translocation. *Proc. Natl. Acad. Sci. USA.* 74:3119–3123.

van der Meer, K., J. J. C. Mulder, and J. Lugtenberg. 1976. A new facet in rhodopsin photochemistry. *Photochem. Photobiol.* 24:363–367.

Warshel, A. 1978. Charge stabilization mechanism in the visual and purple membrane pigments. *Proc. Natl. Acad. Sci. USA.* 75:2558–2562.

Yu, W., F. Pellegrino, M. Grout, and R. R. Alfano. 1977. Subnanosecond fluorescence quenching of dye molecules in solutions. *J. Chem. Phys.* 67:1766–1773.